International Journal of Mass Spectrometry 190/191 (1999) 243–251

Gas phase ion chemistry in silane/propane and silane/propene mixtures

P. Antoniotti, L. Operti, R. Rabezzana, G.A. Vaglio*, P. Volpe

Dipartimento di Chimica Generale ed Organica Applicata, Università di Torino, Corso Massimo d'Azeglio 48, 10125 Torino, Italy

Received 13 October 1998; accepted 21 January 1999

Abstract

The silane/propane and silane/propene gaseous mixtures have been investigated by ion trap mass spectrometry. The variations of ion abundances observed under different partial and total pressures are reported. The mechanisms of ion/molecule reactions have been elucidated by successive isolation steps. Moreover, the rate constants for the main processes have been experimentally measured and compared with the collisional rate constants to determine the reaction efficiencies. A great number of processes have been observed in SiH_4/C_3H_6 leading to the formation of silicon and carbon containing ions with high efficiency, whereas propane and silane give very few ion products with low efficiencies. Chain propagation in the SiH_4/C_3H_6 system gives clusters of increasing size, such as $Si_2C_2H_7^+$ and $Si_3CH_7^+$, with rather high efficiencies starting from silicon containing ions and neutral propene. (Int J Mass Spectrom 190/191 (1999) 243–251) © 1999 Elsevier Science B.V.

Keywords: Propane; Propene; Silane; Ion trap mass spectrometry; Kinetics

1. Introduction

Gas phase ion chemistry is a research field in continuous development because of the strong interest, both fundamental and applicative, in the study of reactivity, mechanisms, and kinetics of isolated species [1–3]. In fact, such studies allow one to obtain information about the intrinsic behavior of ions in the absence of perturbations due to solvent or counterions [4–12] and give the possibility of direct correlation with ab initio quantum chemical calculations on the relative stability of ion structures, reaction energetic profiles, and thermochemical data [13–16]. This research also has a remarkable importance in astrochemistry providing reliable modeling for the reactivity of ions and molecules in interstellar clouds [17–19]; in the study of plasmas and, in general, for the planning of new materials by deposition from gas mixtures suitably activated [7,11,20].

In this respect, an integrated approach, both experimental and theoretical, has been used in the past few years to investigate the gas phase ion chemistry of silane alone. The mechanisms of the chain propagation to form $Si_nH_m^+$ clusters, precursors of amorphous solids obtained by deposition from gaseous mixtures, have been elucidated along with their structures [11,14].

Ion/molecule reactions have also been studied in SiH_4/NH_3 [21] and SiH_4/PH_3 [7] systems under different experimental conditions, with the aim of investigating the formation of ion species containing new Si–N and Si–P bonds and of simulating the design of

---

* Corresponding author.

Dedicated to J.F.J. Todd and R.E. March in recognition of their original contributions to quadrupole ion trap mass spectrometry.

PII S1387-3806(99)00024-X

amorphous silicon doped with elements from group 15 of the periodic system.

In this article we report on the mechanisms and kinetics of ion/molecule reactions in the SiH_4/C_3H_8 and SiH_4/C_3H_6 systems studied by ion trap mass spectrometry. The results offer insights on silicon fundamental chemistry and investigate the main factors affecting the formation of silicon and carbon containing ions that may be considered charged precursors in the deposition of amorphous films of silicon carbides. The rate constants of the main ion/molecule reactions have also been experimentally determined and compared with the collisional rate constants calculated according to the Langevin or ADO (average dipole orientation) theories [22].

2. Experimental

Silane, propane, and propene were obtained commercially in high purity. Each was introduced into a flask containing anhydrous sodium sulfate as a drier, that was connected to one line of the gas inlet system of the instrument. Helium was supplied at an extra-high purity degree and used without further purification. All experiments were run on an ITMS Finnigan mass spectrometer. A Bayard Alpert ionization gauge was used to measure pressure. The read pressures were corrected for the relative sensitivity of the ion gauge with respect to different gases [23,24] and for a calibration factor, calculated as reported previously [5], to obtain the real pressure in the trap. Helium buffer gas was admitted into the trap at a pressure of $\sim 4 \times 10^{-4}$ Torr (1 Torr $=$ 133 Pa). The temperature of the trap was maintained at 333 K, a temperature at which other related systems have been studied. In all experiments ions were detected in the 10–300 u mass range. In order to prevent side reactions with water background, the manifold and the lines for introduction of reagent gases and helium were frequently baked up. In these experiments, the scan modes used both to study the overall ion reactivity as a function of time and to determine reaction mechanisms and rate constants have been described in detail previously, as have the procedures for calculations [5,7,13].

In the kinetic experiments the isolation of ions at a specific *m/z* value was obtained by use of dc voltages and by resonance ejection, as described previously [13]. In the latter isolation method no field is directly applied to the selected ionic species and, therefore, the ions should have a lower excitation energy. The rate constants obtained by using these two different isolation procedures are very similar. This is in agreement with the hypothesis that the reactant ions undergo a number of collisions sufficient to eliminate most of their excitation energy. The single exponential decays observed in the kinetic experiments are consistent with this hypothesis.

In all experiments ionization was obtained by electron impact for times in the range 1–10 ms. In experiments without selective storage of ions, ionization is followed by a reaction time, which ranges from 0–500 ms, without application of any potential to the trap. Acquisition of ion signal closes the experiment. When isolation of an ion species is performed, after the ionization event, a reaction time follows in order to maximize the abundances of the ions under examination. Isolation of the selected ions, storage in the trap for convenient reaction times, and acquisition are the successive events.

In some cases, when it was impossible to identify the neutral reagent (i.e. $SiCH_4^+$ giving $SiCH_5^+$), experiments were performed by pulsing one of the reagent gases into the trap and studying the reaction paths after it was pumped away. A General Valve Corporation Iota One pulsed valve (Fairfield, NJ) was used [25]. Fig. 1 shows the pulsed gas profile, i.e. the trend of its ion current as a function of elapsed time since the valve has been triggered. The pressure of the pulsed gas behind the valve has been set previously at 1.0×10^{-6} Torr by means of a bypass channel. The profile is ~1.5 s wide. The valve opening time is 0.25 ms; the pulsed gas pressure has a rise time of about 250 ms, reaches a maximum, and is pumped away by a turbomolecular pump in about 1500 ms.

3. Results and discussion

3.1. Silane/propane mixtures

The trends of the abundances of all the ion families containing both silicon and carbon at total pressures

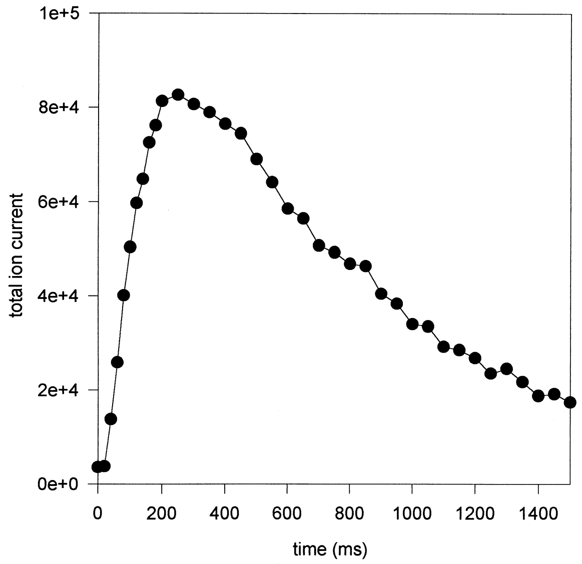

Fig. 1. Variation of the total ion current of propene introduced into the ion trap through a pulsed valve as a function of elapsed time since the valve has been triggered.

of 5.0 × 10^{-7} and 1.5 × 10^{-6} Torr, as a function of time, are shown in Figs. 2 and 3. In each figure the plots are reported for three mixtures with 1:1, 1:5, and 5:1 ratios of partial pressure of silane and propane, with the aim of studying the experimental conditions that favor the formation of Si–C bonds. The ion abundances in the 1:5 silane/propane systems show a similar behavior at the two different total pressures, whereas they continuously increase with time in the presence of silane excess. The 1:1 mixture displays an intermediate behavior because the ion abundances increase up to 300 ms reaction time and then remain constant (5.0 × 10^{-7} Torr total pressure) or continuously increase (1.5 × 10^{-6} Torr total pressure). Regardless, the 5:1 SiH_4/C_3H_8 system gives the highest yield of ions containing silicon and carbon at both total pressures.

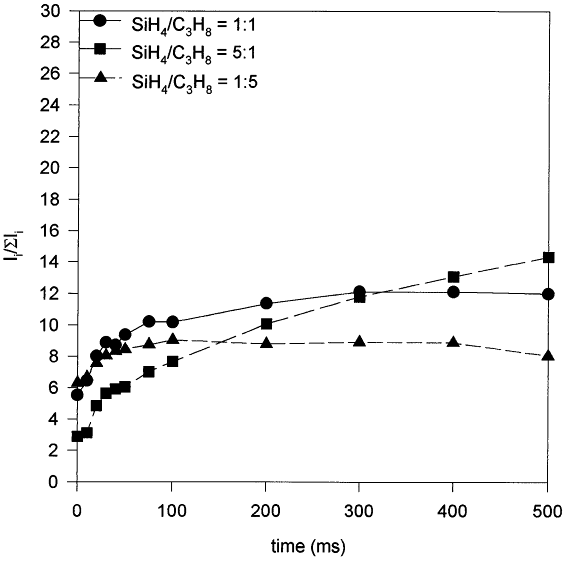

Fig. 2. Variation of total abundances with time for silicon and carbon containing ions in SiH_4/C_3H_8 mixtures at 5.0 × 10^{-7} Torr total pressure.

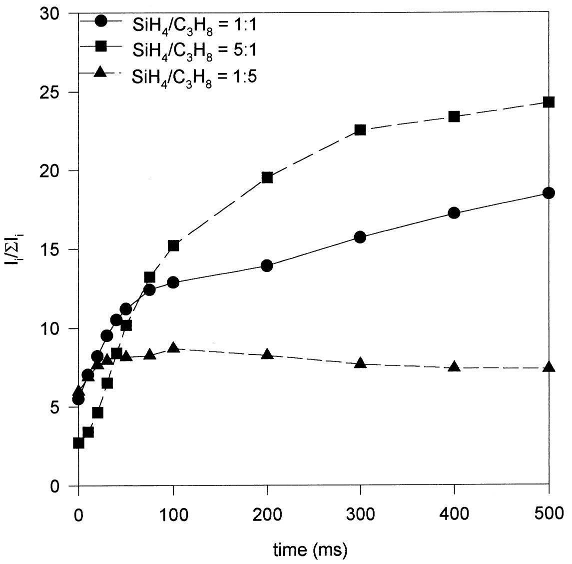

Fig. 3. Variation of total abundances with time for silicon and carbon containing ions in SiH_4/C_3H_8 mixtures at 1.5 × 10^{-6} Torr total pressure.

Table 1 reports the most important ion/molecule reactions occurring in SiH_4/C_3H_8 mixtures together with the experimental rate constants for the formation of ionic products. The collisional rate constants are calculated according to the Langevin theory for silane [26] and propane [27] as well. In fact, as far as this latter molecule is concerned, its dipole moment is so low (0.084 Debye [27]) as to make the second part of the ADO equation negligible. It follows that the ADO equation becomes equal to the Langevin one. The

Table 1
Rate constants for reactions of $C_3H_n^+$, SiH_3^+, and $SiCH_5^+$ ions in a SiH_4/C_3H_8 mixture[a]

Reaction	k_{exp}	Σk_{exp}	k_L[b]	Efficiency[c]
$C_3H_3^+ + C_3H_8 \rightarrow C_3H_7^+ + C_3H_4$	2.1			
$\rightarrow C_4H_7^+ + C_2H_4$	0.62	2.7	12.90	0.21
$C_3H_3^+ + SiH_4 \rightarrow SiCH_3^+ + C_2H_4$	0.30			
$\rightarrow SiCH_5^+ + C_2H_2$	1.6	1.9	11.61	0.16
$C_3H_5^+ + C_3H_8 \rightarrow C_3H_7^+ + C_3H_6$	2.7	2.7	12.73	0.21
$C_3H_5^+ + SiH_4 \rightarrow SiCH_5^+ + C_2H_4$	4.4	4.4	11.48	0.38
$SiH_3^+ + C_3H_8 \rightarrow C_3H_7^+ + SiH_4$	11	11	13.74	0.80
$SiCH_5^+ + SiH_4 \rightarrow Si_2H_5^+ + CH_4$	0.51	0.51	11.25	0.045

[a] Rate constants are expressed as 10^{-10} cm^3 molecule^{-1} s^{-1}; experiments were run at 333 K; uncertainty is within 20%.
[b] Rate constants have been calculated according to the Langevin theory taking polarizability of SiH_4 from [26] and of C_3H_8 from [27].
[c] Efficiency has been calculated as the ratio $\Sigma k_{exp}/k_L$.

reaction efficiencies are reported as the ratio of experimental to collisional rate constants. The self-condensation processes of silane, occurring as parallel reactions of the reported pathways, have already been published [5,21] and are not shown for reasons of clarity. Some of the ion/molecule reactions occurring in the SiH_4/C_3H_8 mixture produce ions such as $Si_2CH_n^+$ ($n = 5$–7) and $Si_2C_2H_6^+$, which are not reported in the table because of the very low abundance of the product ions, that makes it impossible to determine the reaction rate constants with good reproducibility.

Among SiH_n^+ ($n = 0$–3) ions only SiH_3^+ reacts with propane by hydride abstraction to produce the $C_3H_7^+$ ion, whereas SiH_n^+ ($n = 0$–2) ion species are unreactive in the delay time considered. The $C_3H_n^+$ ($n = 3, 5$) ions react with silane yielding the $SiCH_n^+$ ($n = 3, 5$) ion species, with an appreciable overall rate constant for $n = 5$. These processes take place with substitution of a small molecule (i.e. C_2H_2 or C_2H_4) by silane and become exothermic according to the heats of formation reported in the literature [28–30]. Formation of larger mixed ion clusters, i.e. species containing silicon and carbon, does not proceed further because $SiCH_3^+$ is unreactive in the experimental conditions used here, and in $SiCH_5^+$ ions the carbon is replaced by a silicon atom to give $Si_2H_5^+$ from reaction with silane. The $C_3H_n^+$ ions also react in self-condensation processes to produce $C_4H_7^+$ and $C_3H_7^+$, their rate constants being in the same order of magnitude as those of the reactions with silane. It clearly appears that the silane/propane mixtures do not favor the formation of large mixed clusters through ion/molecule reactions.

3.2. Silane/propene mixtures

The variations of the abundances of all the ion species containing both silicon and carbon, as a function of reaction time, for three SiH_4/C_3H_6 systems (1:1, 1:5, and 5:1 ratios of partial pressure of the two reagents) are reported at the total pressure of 5.0×10^{-7} and 1.5×10^{-6} Torr in Figs. 4 and 5, for the interest in the formation of cluster ions of silicon and carbon. All three silane/propene systems show remarkably higher relative abundances of Si–C containing ions with respect to silane/propane systems under the same conditions. Moreover, at 1.5×10^{-6} Torr pressure (Fig. 5) the 1:1 SiH_4/C_3H_6 mixture displays the highest ion abundances, continuously increasing with time. A lower increase is shown by the mixture containing an excess of silane at the same total pressure. In this case the highest yield of ions containing silicon and carbon is observed in the mixture with equal amounts of the two reagent gases. Such behavior indicates a higher involvement of propene with respect to propane in the formation of mixed ion clusters.

In Tables 2, 3, 4, and 5 the ion/molecule reactions occurring in a SiH_4/C_3H_6 system, together with the experimental and collisional rate constants (Langevin and ADO theories [22]) and the reaction efficiencies,

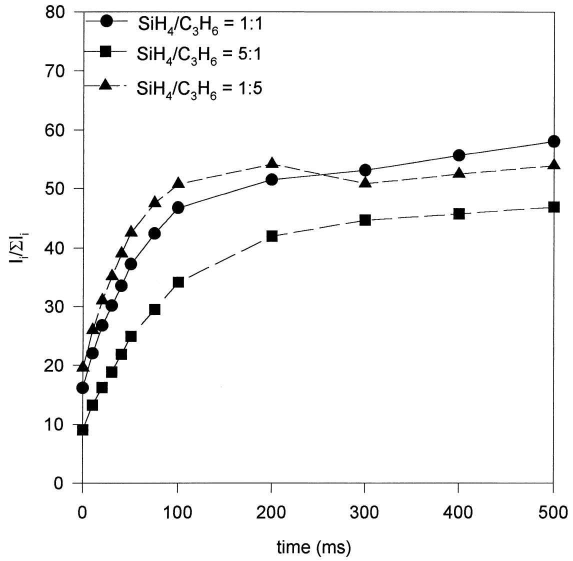

Fig. 4. Variation of total abundances with time for silicon and carbon containing ions in SiH_4/C_3H_6 mixtures at 5.0×10^{-7} Torr total pressure.

are reported. Table 2 shows the ion/molecule reactions of the silane primary ions with C_3H_6. The kinetics of the Si^+ ion were not studied because that ion has the same nominal mass as the propene fragment ion $C_2H_4^+$ (m/z = 28). Table 3 reports the reactions of the secondary ions of silane, $Si_2H_n^+$ (n = 2–5), with C_3H_6, and Table 4 reports those of the primary ions of propene, $C_2H_3^+$ and $C_3H_n^+$ (n = 1–7) with both silane and propene. Finally, Table 5 shows the ion/molecule reactions of $SiCH_n^+$ (n = 4, 5), $SiC_2H_5^+$, $SiC_3H_7^+$, and $Si_2CH_5^+$ ions with both silane and propene. The great number of reactions leading to the formation of mixed ions, containing both silicon and carbon, together with their rather high rate constants, indicates that the SiH_4/C_3H_6 system is suitable for the preparation of amorphous silicon carbides.

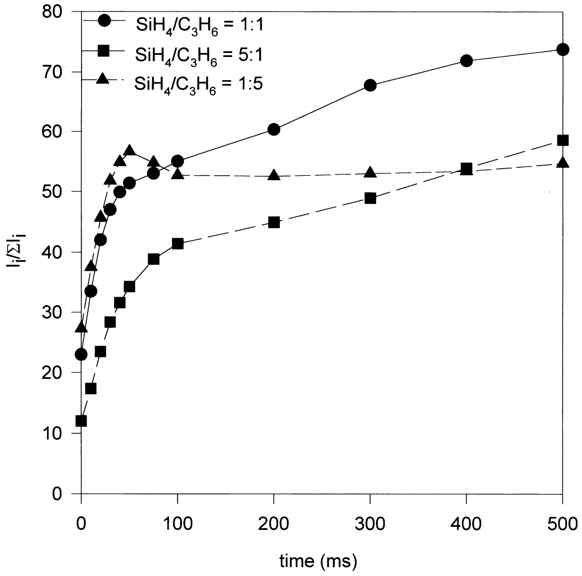

Fig. 5. Variation of total abundances with time for silicon and carbon containing ions in SiH_4/C_3H_6 mixtures at 1.5×10^{-6} Torr total pressure.

The most common pathway displayed by the SiH_n^+ (n = 1–3) ions reacting with C_3H_6 occurs with loss of a C_2H_4 molecule, its rate constants being rather high. The SiH^+ and SiH_2^+ ions also react in different pathways with loss of a variety of neutral fragments. In particular, SiH_2^+ yields $SiC_3H_7^+$, and this is the only case in which no carbon containing fragment is lost.

The $Si_2H_n^+$ ions show a good reactivity towards propene, as shown by the many reactions with appreciable rate constants. Also, in this case, elimination of a C_2H_4 molecule is a pathway frequently observed. Substitution of a SiH_4 by a C_3H_6 molecule is also displayed by the $Si_2H_4^+$ and $Si_2H_5^+$ ions. Moreover, the $Si_2H_2^+$ ion species undergo a considerable number of reactions with C_3H_6 yielding, among others, the quite large cluster $Si_2C_3H_7^+$.

Calculated reaction enthalpies [28,29,31] for the reactions starting from the SiH_n^+ (n = 1–3) ions are negative. Among processes of silane secondary ions, thermochemical data were available only for the reaction of $Si_2H_3^+$, which turned out to be negative too [28,31,32].

The $C_nH_m^+$ ions react in self-condensation processes through many different pathways. In some cases, large ions containing up to six carbon atoms are observed, but these product ions are unreactive in the experimental conditions used here. Again, elimination of C_2H_4 as a neutral product is a common path. Calculation of the energetics of these processes, considering the most stable isomer for each ion [28], gives reaction enthalpies that are generally negative. The only exception is the reaction $C_3H_2^+ + C_3H_6 \rightarrow$

Table 2
Rate constants for reactions of SiH_n^+ ions with C_3H_6 in a SiH_4/C_3H_6 mixture[a]

Reaction	k_{exp}	Σk_{exp}	k_{ADO}[b]	Efficiency[c]
$SiH^+ + C_3H_6 \rightarrow SiH_3^+ + C_3H_4$	0.84			
$\rightarrow SiCH_3^+ + C_2H_4$	9.5			
$\rightarrow SiCH_5^+ + C_2H_2$	3.0	13.3	14.88	0.89
$SiH_2^+ + C_3H_6 \rightarrow SiCH_4^+ + C_2H_4$	7.9			
$\rightarrow SiCH_5^+ + C_2H_3$	5.0			
$\rightarrow SiC_2H_5^+ + CH_3$	1.3			
$\rightarrow SiC_2H_6^+ + CH_2$	1.3			
$\rightarrow SiC_3H_7^+ + H$	1.0	16.5	14.74	1.12
$SiH_3^+ + C_3H_6 \rightarrow SiCH_5^+ + C_2H_4$	15	15	14.60	1.03

[a] Rate constants are expressed as 10^{-10} cm^3 $molecule^{-1}$ s^{-1}; experiments were run at 333 K; uncertainty is within 20%.
[b] Rate constants have been calculated according to the ADO theory taking the polarizability and dipole moment of C_3H_6 from [27].
[c] Efficiency has been calculated as the ratio $\Sigma k_{exp}/k_{ADO}$.

$C_4H_4^+ + C_2H_4$, which is endothermic by about 16 kcal $molecule^{-1}$.

Reactions of $C_nH_m^+$ ions with silane (Table 4) generally take place through a smaller number of pathways with respect to propene. Addition of a SiH_4 molecule followed by loss of a fragment containing one or two carbon atoms is very frequent, and loss of hydrogen is also observed in a few cases, leading to the formation of $SiC_2H_5^+$, $SiC_3H_2^+$, $SiC_3H_3^+$, and $SiC_3H_8^+$ ions. Negative reaction enthalpies have been calculated for all processes in Table 4 [28,33–35], except those producing $SiC_3H_2^+$ and $SiC_3H_8^+$ because their heats of formation are not available in the literature. As far as formation of $SiC_2H_7^+$ ion is concerned, the heat of formation is available for the $Si(CH_3)_2H^+$ structure [33], which is reported to be the most stable $SiC_2H_7^+$ isomer [36], on the basis of ab initio calculations.

Mixed clusters react with both C_3H_6 and SiH_4 in an appreciable number of pathways (Table 5), even if reaction efficiencies are often quite low. Again, in reactions with C_3H_6, the most frequent path takes place with loss of a C_2H_4 molecule and it generally displays the highest rate constants. On the other hand, reactions with silane are mainly followed by loss of a hydrogen or a methane molecule. Moreover, it is worth noting that mixed ions show higher reaction efficiencies with propene rather than with silane.

Table 3
Rate constants for reactions of $Si_2H_n^+$ ions with C_3H_6 in a SiH_4/C_3H_6 mixture[a]

Reaction	k_{exp}	Σk_{exp}	k_{ADO}[b]	Efficiency[c]
$Si_2H_2^+ + C_3H_6 \rightarrow Si_2H_3^+ + C_3H_5$	1.5			
$\rightarrow SiC_3H_5^+ + SiH_3$	1.1			
$\rightarrow Si_2CH_4^+ + C_2H_4$	2.9			
$\rightarrow Si_2C_2H_5^+ + CH_3$	2.8			
$\rightarrow Si_2C_3H_7^+ + H$	1.6	9.9	12.49	0.79
$Si_2H_3^+ + C_3H_6 \rightarrow Si_2CH_5^+ + C_2H_4$	5.8	5.8	12.45	0.47
$Si_2H_4^+ + C_3H_6 \rightarrow SiC_3H_6^+ + SiH_4$	1.5			
$\rightarrow SiC_3H_7^+ + SiH_3$	2.1			
$\rightarrow Si_2CH_5^+ + C_2H_5$	1.1			
$\rightarrow Si_2CH_6^+ + C_2H_4$	4.4	9.1	12.40	0.73
$Si_2H_5^+ + C_3H_6 \rightarrow SiC_3H_7^+ + SiH_4$	0.74			
$\rightarrow Si_2CH_7{}^+ + C_2H_4$	5.2	5.9	12.36	0.48

[a] Rate constants are expressed as 10^{-10} cm^3 $molecule^{-1}$ s^{-1}; experiments were run at 333 K; uncertainty is within 20%.
[b] Rate constants have been calculated according to the ADO theory taking the polarizability and dipole moment of C_3H_6 from [27].
[c] Efficiency has been calculated as the ratio $\Sigma k_{exp}/k_{ADO}$.

Table 4
Rate constants for reactions of $C_2H_3^+$ and $C_3H_n^+$ ions in a SiH_4/C_3H_6 mixture[a]

Reaction	k_{exp}	Σk_{exp}	$k_{L/ADO}$[b]	Efficiency[c]
$C_2H_3^+ + C_3H_6 \rightarrow C_3H_5^+ + C_2H_4$	4.6	4.6	15.21	0.30
$C_2H_3^+ + SiH_4 \rightarrow SiH_3^+ + C_2H_4$	2.8			
$\rightarrow SiC_2H_5^+ + H_2$	0.59	3.4	12.72	0.27
$C_3H^+ + C_3H_6 \rightarrow C_2H_3^+ + 2C_2H_2$	1.3			
$\rightarrow C_3H_3^+ + C_3H_4$	1.8			
$\rightarrow C_4H_3^+ + C_2H_4$	3.4	6.5	13.91	0.47
$C_3H^+ + SiH_4 \rightarrow SiCH_3^+ + C_2H_2$	5.9			
$\rightarrow SiC_3H_2^+ + H_2 + H$	1.4			
$\rightarrow SiC_3H_3^+ + H_2$	2.4	9.7	11.75	0.82
$C_3H_2^+ + C_3H_6 \rightarrow C_3H_3^+ + C_3H_5$	0.88			
$\rightarrow C_3H_5^+ + C_3H_3$	0.56			
$\rightarrow C_4H_4^+ + C_2H_4$	0.88			
$\rightarrow C_5H_5^+ + CH_3$	3.4			
$\rightarrow C_6H_5^+ + H_2 + H$	2.6			
$\rightarrow C_6H_7^+ + H$	2.4	10.7	13.81	0.78
$C_3H_2^+ + SiH_4 \rightarrow SiCH_3^+ + C_2H_3$	1.8			
$\rightarrow SiCH_4^+ + C_2H_2$	0.64			
$\rightarrow SiC_2H_3^+ + CH_3$	1.8			
$\rightarrow SiC_3H_3^+ + H_2 + H$	1.1	5.3	11.68	0.45
$C_3H_3^+ + C_3H_6 \rightarrow C_4H_5^+ + CH_3$	0.55	0.55	13.72	0.040
$C_3H_3^+ + SiH_4 \rightarrow SiCH_3^+ + C_2H_4$	0.42			
$\rightarrow SiCH_5^+ + C_2H_2$	1.2	1.6	13.72	0.12
$C_3H_4^+ + C_3H_6 \rightarrow C_3H_6^+ + C_3H_4$	0.47			
$\rightarrow C_4H_6^+ + C_2H_4$	1.1			
$\rightarrow C_5H_7^+ + CH_3$	7.2			
$\rightarrow C_6H_9^+ + H$	0.45	9.2	13.63	0.68
$C_3H_4^+ + SiH_4 \rightarrow SiCH_4^+ + C_2H_4$	0.50	0.50	11.54	0.043
$C_3H_5^+ + C_3H_6 \rightarrow C_4H_7^+ + C_2H_4$	7.7	7.7	13.54	0.56
$C_3H_5^+ + SiH_4 \rightarrow SiCH_5^+ + C_2H_4$	4.8	4.8	11.48	0.42
$C_3H_6^+ + C_3H_6 \rightarrow C_3H_7^+ + C_3H_5$	3.6			
$\rightarrow C_4H_7^+ + C_2H_5$	0.85			
$\rightarrow C_4H_8^+ + C_2H_4$	4.1			
$\rightarrow C_5H_9^+ + CH_3$	2.2	10.8	13.46	0.80
$C_3H_6^+ + SiH_4 \rightarrow SiC_2H_7^+ + CH_3$	6.8			
$\rightarrow SiC_3H_8^+ + H_2$	3.2	10	11.42	0.88
$C_3H_7^+ + C_3H_6 \rightarrow C_4H_9^+ + C_2H_4$	1.8	1.8	13.38	0.13
$C_3H_7^+ + SiH_4 \rightarrow SiC_2H_7^+ + CH_4$	0.73			
$\rightarrow SiC_3H_9^+ + H_2$	0.29	1.0	11.36	0.090

[a] Rate constants are expressed as 10^{-10} cm^3 $molecule^{-1}$ s^{-1}; experiments were run at 333 K; uncertainty is within 20%.

[b] Rate constants have been calculated according to the Langevin theory for reactions of SiH_4 and the ADO theory for reactions of C_3H_6, taking polarizabilities from [26] and [27], respectively, and the dipole moment of C_3H_6 from [27].

[c] Efficiency has been calculated as the ratio $\Sigma k_{exp}/k_L$ or $\Sigma k_{exp}/k_{ADO}$.

Exothermicity of ion/molecule reactions reported in Table 5 has been checked [28,32,34,37] for the processes that do not involve, as either product or reagent, the $Si_2CH_6^+$, $SiC_3H_6^+$, $SiC_5H_6^+$, $Si_2C_2H_7^+$, $Si_3CH_7^+$ ions, whose formation enthalpies are not available. As far as the $SiC_3H_9^+$ ion is concerned, the heat of formation of the $(CH_3)_3Si^+$ isomer has been used [33], because is to considered the most stable one [36,38,39].

The $SiCH_4^+$ ion reacts in the SiH_4/C_3H_6 mixture to give $SiCH_5^+$ and it has been observed that this hydrogenation process occurs with both C_3H_6 and SiH_4. Heats of formations [28,29] indicate that the reaction with propene is thermodynamically more

Table 5
Rate constants for reactions of $SiCH_n^+$, $SiC_2H_5^+$, $SiC_3H_7^+$, and $Si_2CH_5^+$ ions in a SiH_4/C_3H_6 mixture[a]

Reaction	k_{exp}	Σk_{exp}	$k_{L/ADO}$[b]	Efficiency[c]
$SiCH_4^+ + C_3H_6 \rightarrow SiCH_5^+ + C_3H_5$	2.2			
$\rightarrow SiC_2H_6^+ + C_2H_4$	5.0			
$\rightarrow SiC_2H_7^+ + C_2H_3$	1.7	8.9	13.30	0.67
$SiCH_4^+ + SiH_4 \rightarrow SiCH_5^+ + SiH_3$	3.5			
$\rightarrow Si_2H_2^+ + CH_4 + H_2$	0.94			
$\rightarrow Si_2H_3^+ + CH_4 + H$	1.6			
$\rightarrow Si_2CH_6^+ + H_2$	0.70	6.7	11.30	0.60
$SiCH_5^+ + C_3H_6 \rightarrow SiC_2H_7^+ + C_2H_4$	8.4	8.4	13.23	0.63
$SiCH_5^+ + SiH_4 \rightarrow Si_2H_5^+ + CH_4$	0.65	0.65	11.25	0.058
$SiC_2H_5^+ + C_3H_6 \rightarrow SiC_3H_7^+ + C_2H_4$	6.6			
$\rightarrow SiC_5H_9^+ + H_2$	0.40	7.0	12.54	0.56
$SiC_2H_5^+ + SiH_4 \rightarrow Si_2H_3^+ + C_2H_6$	0.70			
$\rightarrow Si_2CH_5^+ + CH_4$	0.25	0.95	10.75	0.088
$SiC_3H_7^+ + C_3H_6 \rightarrow SiC_4H_9^+ + C_2H_4$	5.0			
$\rightarrow SiC_6H_{11}^+ + H_2$	0.40	5.4	12.00	0.45
$SiC_3H_7^+ + SiH_4 \rightarrow Si_2H_5^+ + C_3H_6$	0.67	0.67	10.36	0.065
$Si_2CH_5^+ + C_3H_6 \rightarrow Si_2C_2H_7^+ + C_2H_4$	2.1	2.1	11.94	0.18
$Si_2CH_5^+ + SiH_4 \rightarrow Si_3H_5^+ + CH_4$	0.25			
$\rightarrow Si_3CH_7^+ + H_2$	0.13	0.38	10.32	0.037

[a] Rate constants are expressed as 10^{-10} cm^3 $molecule^{-1}$ s^{-1}; experiments were run at 333 K; uncertainty is within 20%.

[b] Rate constants have been calculated according to the Langevin theory for reactions of SiH_4 and the ADO theory for reactions of C_3H_6, taking polarizabilities from [26] and [27], respectively, and dipole moment of C_3H_6 [27].

[c] Efficiency has been calculated as the ratio $\Sigma k_{exp}/k_L$ or $\Sigma k_{exp}/k_{ADO}$.

favored than with silane. However, some experiments have been performed pulsing one reacting gas and leaking the other at a constant pressure into the trap. The introduction of a gas through a pulsed valve allows one to have a variable gas pressure during the experiment time. In fact, after the valve has been opened for a suitable time, the pressure of a pulsed gas increases, reaches a maximum, and then decreases as a consequence of the fact that the trap is continuously evacuated. In our experiments, the ionization event took place while the pressure of the gas was at the top, and the selected ion was reacted when the pulsed gas was already pumped off the trap. Therefore, the $SiCH_4^+$ ion was formed, selected, and reacted with just one neutral at a time. Two different experiments, performed pulsing C_3H_6 and SiH_4 alternatively, allowed us to determine that both neutrals originate the $SiCH_5^+$ ion. The rate constants indicate that the reaction with silane proceeds faster than with propene. This is probably because of the lower Si–H bond energy with respect to the C–H one [40], which determines an activation complex of lower energy in the reaction of SiH_4 with respect to C_3H_6. Besides, in both experiments product ions at nominal mass of 58 and 59 have been detected. When the neutral reagent is C_3H_6, the formulae $SiC_2H_6^+$ and $SiC_2H_7^+$ can be respectively assigned to these ions. In the other case, the formed ions can be assumed to be $Si_2H_2^+$ and $Si_2H_3^+$.

4. Conclusions

From the comparison of the two systems examined here, it is evident that the silane/propene mixture is the most suitable for the formation and growth of silicon and carbon containing ion clusters, as possible precursors of amorphous silicon carbides. In fact, a general higher reactivity of propene with respect to propane is observed, as evidenced by the great number of reactions occurring at appreciable rates, and by the ions formed. Such processes take place between hydrocarbon ions and silane or silicon containing ions and propene and produce mixed ions of increasing size. Moreover, an improved yield of mixed ion clusters is given by increasing the total pressure of reagent gases, in particular in the 1:1 SiH_4/C_3H_6 mixture.

Acknowledgements

The authors thank Ministero dell'Università e della Ricerca Scientifica e Tecnologica and Università di Torino for financial support.

References

[1] N.G. Adams, L.M. Babcock, Advances in Gas Phase Ion Chemistry, Jai, Greenwich, 1996, Vol. 2.
[2] F. Cacace, Pure Appl. Chem. 69 (1997) 227.
[3] D. Schröder, C. Heinemann, W. Koch, H. Schwarz, Pure Appl. Chem. 69 (1997) 273.
[4] P. Benzi, L. Operti, G.A. Vaglio, P. Volpe, M. Speranza, R. Gabrielli, Int. J. Mass Spectrom. Ion Processes 100 (1990) 647.
[5] L. Operti, M. Splendore, G.A. Vaglio, A.M. Franklin, J.F.J. Todd, Int. J. Mass Spectrom. Ion Processes 136 (1994) 25.
[6] P. Benzi, L. Operti, R. Rabezzana, M. Splendore, P. Volpe, Int. J. Mass Spectrom. Ion Processes 152 (1996) 61.
[7] P. Antoniotti, L. Operti, R. Rabezzana, G.A. Vaglio, P. Volpe, J.F. Gal, R. Grover, P.C. Maria, J. Phys. Chem. 100 (1996) 155.
[8] F. Cacace, M. Speranza, Science 265 (1994) 208.
[9] M.T. Bowers, A.G. Marshall, F.W. McLafferty, J. Phys. Chem. 100 (1996) 12 897.
[10] I. Haller, J. Phys. Chem. 94 (1990) 4135.
[11] W.D. Reents Jr., M.L. Mandich, J. Chem. Phys. 96 (1992) 4429.
[12] J. Berkowitz, L.A. Curtiss, S.T. Gibson, J.P. Greene, G.L. Hillhouse, J.A. Pople, J. Chem. Phys. 84 (1986) 375.
[13] P. Antoniotti, L. Operti, R. Rabezzana, M. Splendore, G. Tonachini, G.A. Vaglio, J. Chem. Phys. 107 (1997) 1491.
[14] K. Raghavachari, J. Chem. Phys. 96 (1992) 4440.
[15] E.M. Cruz, X. Lopez, M. Ayerbe, J.M. Ugalde, J. Phys. Chem. 101 (1997) 2166.
[16] E.M. Cruz, X. Lopez, M. Sarobe, F.P. Cossío, J.M. Ugalde, J. Comput. Chem. 18 (1997) 9.
[17] S. Petrie, H. Becker, V. Baranov, D.K. Bohme, Astrophys. J. 476 (1997) 191.
[18] S. Petrie, D.K. Bohme, Astrophys. J. 436 (1994) 411.
[19] S. Petrie, D.K. Bohme, Mon. Not. R. Astron. Soc. 268 (1994) 103.
[20] M. Speranza, Trends Organomet. Chem. 1 (1994) 35.
[21] J.F. Gal, R. Grover, P.C. Maria, L. Operti, R. Rabezzana, G.A. Vaglio, P. Volpe, J. Phys. Chem. 98 (1994) 11 978.
[22] M.T. Bowers, Gas Phase Ion Chemistry, Academic, New York, 1979, Vol. 1.
[23] M. Decouzon, J.F. Gal, P.C. Maria, A.S. Tchinianga, personal communication.
[24] J.E. Bartmess, R.M. Georgiadis, Vacuum 33 (1983) 149.
[25] T.J. Carlin, B.S. Freiser, Anal. Chem. 55 (1983) 571.
[26] E.R. Lippincott, J.M. Stutman, J. Phys. Chem. 78 (1974) 2422.
[27] A.A. Maryott, F. Buckley, U.S. National Bureau of Standards Circular No. 537, (1953).
[28] S.G. Lias, J.E. Bartmess, J.F. Liebman, J.L. Holmes, R.D. Levin, W.G. Mallard, J. Phys. Chem. Ref. Data 17 (1988) (suppl.).
[29] R. Bakhtiar, C.M. Holznagel, D.B. Jacobson, J. Phys. Chem. 97 (1993) 12 710.
[30] B.H. Boo, J.L. Elkind, P.B. Armentrout, J. Am. Chem. Soc. 112 (1990) 2083.
[31] B.H. Boo, P.B. Armentrout, J. Am. Chem. Soc. 109 (1987) 3549.
[32] B.L. Kickel, E.R. Fisher, P.B. Armentrout, J. Phys. Chem. 96 (1992) 2603.
[33] S.K. Shin, R.R. Corderman, J.L. Beauchamp, Int. J. Mass Spectrom. Ion Processes 101 (1990) 257.
[34] B.H. Boo, P.B. Armentrout, J. Am. Chem. Soc. 113 (1991) 6401.
[35] S. Wlodek, A. Fox, D.K. Bohme, J. Am. Chem. Soc. 113 (1991) 4461.
[36] A.E. Ketvirtis, D.K. Bohme, A.C. Hopkinson, Organometallics 14 (1995) 347.
[37] T.M.T. Cheng, T.Y. Yu, F.W. Lampe, J. Phys. Chem. 78 (1974) 1184.
[38] A.E. Ketvirtis, D.K. Bohme, A.C. Hopkinson, J. Mol. Struct.: THEOCHEM 313 (1994) 1.
[39] A.E. Ketvirtis, D.K. Bohme, A.C. Hopkinson, J. Phys. Chem. 98 (1994) 13 225.
[40] K.P. Hubert, G. Herzberg, Molecular Spectra and Molecular Structure Constants of Diatomic Molecules, Van Nostrand, New York, 1979.